Computational investigation of empty nose syndrome

By T. Flint†, M. Esmaily-Moghadam, A. Thamboo‡, N. Velasquez‡ AND P. Moin

1. Motivation and objectives

Empty nose syndrome (ENS) is a rare but debilitating condition commonly resulting from resection of part or all of the inferior turbinate (Figure 1). The characteristic yet most perplexing symptom of ENS is the complaint of nasal obstruction despite objectively patent airways, termed paradoxical nasal obstruction. As benign as it sounds, the feeling of obstruction to nasal breathing can have a significant influence on patients' well-being and cannot be remedied simply by instruction to breathe through the mouth. Patients feel constant discomfort during breathing and often get a feeling of mild suffocation which can result in symptoms such as irritability, exhaustion, or anxiety. Furthermore, ENS often occurs in patients suffering from atrophic rhinitis (AR). There has been debate as to whether ENS is a form of AR or a separate entity in itself, but many patients with ENS also present symptoms such as nasal crusting or malodor inside the nose. Computational fluid dynamics (CFD) offers a unique opportunity to study nasal airflow, allowing the visualization and quantification of airflow characteristics inside the nose. Nasal geometry can be generated from computed tomography (CT) scan data allowing simulation of patient-specific geometries. Little is known about the pathophysiology of ENS, many have speculated; however, few have simulated flow through nasal geometries of patients presenting symptoms of ENS. It has been widely proposed that the paradoxical nasal obstruction is linked to the [lack of] activation of thermoreceptors in the mucous membrane of the nose during convective cooling. It is unknown if symptoms arise out of damage to these receptors or from unfavorable airflow characteristics, but it has been shown that symptoms can be improved through nasal reconstructive surgery. The aims of this work are twofold, to further understand ENS through simulation of patients suffering from the condition, and to develop predictive capability to help determine patients who may be susceptible to ENS after turbinate resection. This information may be used as a surgical planning tool to inform turbinate resection or reconstruction surgery through the use of shape optimization of the interior geometry of the nose. The project remains in its early stages, and an outline of the progress made so far is presented here.

2. Review of the literature

Empty Nose Syndrome (ENS) was first described by Moore and Kern (Moore & Kern 2001) in patients suffering from atrophic rhinitis as characterized by a cavernous nasal airway lacking identifiable turbinate tissue. ENS is caused by trauma or removal of the turbinates and is most common after the resection of the largest of these structures, the inferior turbinate (Chhabra & Houser 2009), in order to relieve nasal obstruction. The

† Department Mechanical Engineering, University of Canterbury, New Zealand
‡ Department of Otolaryngology, School of Medicine, Stanford University, Stanford CA

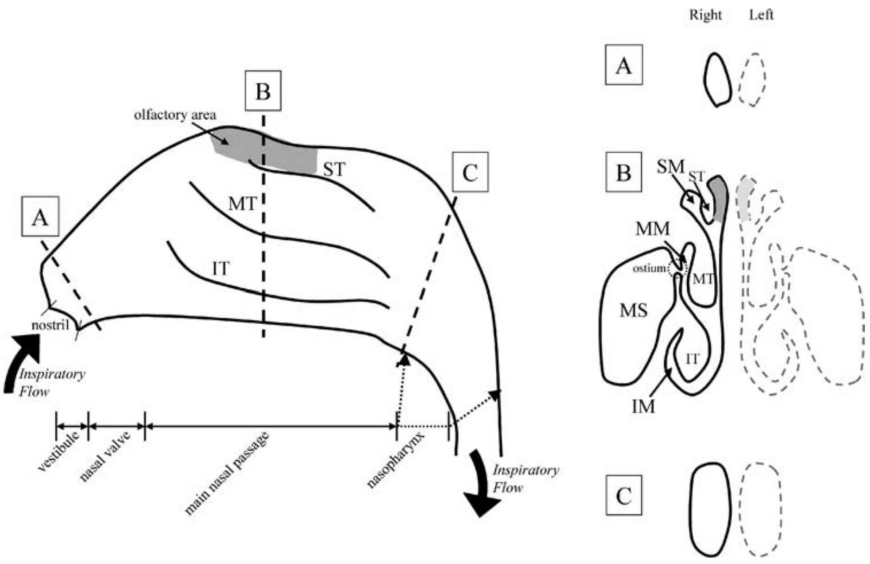

Figure 1: Nasal anatomy adapted from Croce *et al.* (2006). A, B, and C represent cross-sections through the nose. IT, MT, and ST refer to inferior turbinate, middle turbinate, and superior turbinate. IM, MM, and SM refer to inferior meatus, middle meatus, and superior meatus. MS refers to the maxillary sinus. In a patient with ENS, one or several of the turbinates are absent.

actual incidence of ENS is unknown and results seem to vary greatly, but Chharbra & Houser estimated only a 20% incidence following inferior turbinate surgery.

The symptom most characteristic, and most perplexing, of ENS is a subjective sense of paradoxical nasal obstruction. Patients suffering from ENS complain of nasal obstruction or difficulty breathing (dyspnea) despite typical objective tests such as rhinomanometry, acoustic rhinomanometry, and peak nasal inspiratory flow indicating fully patent airways (Houser 2007). Commonly patients display lower than normal nasal resistance. After Houser's landmark paper on the topic (Houser 2007) controversy regarding the classification of ENS followed (Payne 2009). Lack of evidence for the condition led some otolaryngologists to doubt its very existence. As shown by Chhabra & Houser (2009), upon careful investigation of published results on inferior turbinate resection, one does in fact reveal postoperative anomalies such as continued complaints of unexplained breathing difficulty that are indicative of ENS. Further complicating the evidence on ENS, it has been seen that symptoms can take months to years to appear following turbinate surgery (Coste *et al.* 2012). Regardless of its low incidence, ENS can be extremely debilitating for affected individuals, with the difficulty breathing leading to secondary effects such as difficulty concentrating, irritability, and depression (Kuan *et al.* 2015).

The pathophysiology of ENS is not yet fully understood. Recent publications outlining current knowledge on the topic indicate that the cause of ENS appears to be threefold: anatomic changes leading to changes in the airflow patterns in the nose and local environment; disruption of mucosal cooling; and disruption of neurosensory mechanisms governing the sensation of airflow through the nose (Kuan *et al.* 2015).

It is widely accepted that the sensation of nasal patency is related to mucosal cooling

and the activation of the TRPM8 cool thermoreceptors in the nasal mucosa (Zhao *et al.* 2011, 2014). Nerve damage is a risk of any surgery and in some cases the thermoreceptors in one's nose may be damaged following inferior turbinate surgery (Sozansky & Houser 2015). Damage to these thermoreceptors may result in complete loss of functionality in the affected area or just an increased threshold for activation. There is no way to map nerve endings in the human nose, so it is difficult to quantify the extent of nerve damage in an ENS patient's nose. It has, however, been shown that the inferior turbinate is a source for nerve growth factor and its removal could hinder the repair of thermoreceptors following surgery (Wu *et al.* 2006; Sofroniew *et al.* 2001). Tests have indicated that patients with ENS respond with partial relief from nasal congestion upon inhalation of menthol (which directly activates the TRPM8 thermoreceptors) (Freund *et al.* 2011) proving that thermoreceptors are present.

Mucosal cooling is directly linked to the air conditioning capacity of the nose and is responsible for the activation of the cool thermoreceptors. The extent of mucosal cooling is dependent on the nature of the air flow inside the nose and sufficient surface area in contact with fast-flowing air. Patients suffering from ENS have significantly lower surface area-to-volume ratios than those of a healthy person, and simulations have estimated that the turbinates (absent in ENS patients) contribute to 70% of the total air conditioning capacity of a normal nose (Naftali *et al.* 2005). Furthermore, simulations of a patient suffering from ENS reveals significantly reduced air conditioning capacity, with the air remaining cooler and dryer than that in a healthy nose (Garcia *et al.* 2007).

Numerous studies have attempted to visualize the airflow within overly patent airways in order to understand how they differ from a nominal case. Grützenmacher and others (Grützenmacher *et al.* 2003) performed experiments on acrylic casts of a heathy nasal cavity and compared results to that of the same geometry after removal of the inferior turbinate. They found that airflow through the normal nose was quite evenly distributed throughout the entire nasal cavity; however, removal of the inferior turbinate resulted in the majority of air flowing through the lower half of the cavity where the turbinate used to be. Additionally, flow through this region was disorganized, displaying what was described as a strong increase in turbulence. Others corroborated these results with CFD simulations of virtual turbinate removal of healthy nasal geometries derived from CT scans (Di *et al.* 2013; Na *et al.* 2012) showing also that the majority of the air flowed through the bottom half of the cavity. It is interesting to note discrepancy between these results and that of CT models of patients actually suffering from ENS, which found instead that the majority of the airflow travels through the top half of the nasal cavity (Garcia *et al.* 2007; Scheithauer 2010). This indicates that there may be flow features that are unique to ENS and can aid the prediction if this condition through CFD simulation. Studies involving virtual surgery have also investigated how metrics such as nasal resistance and wall shear stress change following inferior turbinate resection, revealing wide variation in results. The work of Wexler and others (Wexler *et al.* 2005) showed a decrease in nasal resistance following removal of the inferior turbinate, Di and others (Di *et al.* 2013) along with Chen and colleagues (Chen *et al.* 2010) found a decrease in nasal resistance as well as wall shear stress. In contrast, Na and others (Na *et al.* 2012) observed increases in both nasal resistance and wall shear stress. These studies demonstrate that airflow patterns following inferior turbinate resection can vary greatly between individuals. All studies of overly patent airways including that of real ENS patients do, however, agree that the airflow in the space formerly occupied by the inferior turbinate is largely disorganized displaying vortical-type structures.

The cotton test (Houser 2007) proves that at least in some cases symptoms of ENS, including paradoxical nasal obstruction, can be partially alleviated by modifications of the internal geometry and hence air-flow characteristics of the nose. Originally used by Houser to judge candidacy for ENS corrective surgery and to plan the size and location of implants, he has also suggested that it be used to aid diagnosis as a confirmatory measure (Chhabra & Houser 2009). The cotton test involves placing cotton that has been moistened with saline solution in the nose where an implant would be feasible. The patient is then asked to breathe normally for 30 minutes and report any changes in his or her symptoms. Only those who notice a definite subjective improvement in their breathing are offered surgery (Houser 2007). Corrective surgical technique has been motivated by the idea of re-establishing nasal resistance, increasing surface area available for air conditioning, and restoring nasal aerodynamics to a nominal state. This has culminated in the goal of restoring turbinate tissue that is absent in ENS (Jang *et al.* 2011). Other suggestions have been made such as ensuring symmetry of the cavities to evenly distribute humidification load (Garcia *et al.* 2007) and to direct airflow to virgin areas of mucosa that have not been damaged by prior surgical abuse (Houser 2007). It is apparent that experience alone cannot guarantee a successful surgical plan, with Houser stating that on occasion he has been surprised by the location of a wad of cotton that gives symptomatic improvement (Houser 2007). It is obvious that more focused CFD analyses are needed if we are to fully understand this condition. Of most relevance to the present study is the work by Garcia and others (Garcia *et al.* 2007) which appears to be the only example of CFD analysis on a patient suffering from ENS before and after surgery to correct the condition. The patient tested also expressed symptoms of atrophic rhinitis (AR) which commonly accompany ENS, and while Garcia and colleagues hypothesized that most symptoms, including crusting and anosmia, could be explained by abnormal water flux distribution causing damage to the mucosa, they were unable to fully explain the cause of the paradoxical nasal obstruction. Their surgery did not relieve the patient of nasal obstruction, but they did speculate that the loss of temperature and pain receptors resulting from the damage to the mucosa may be responsible.

The potential benefits of using CFD to inform nasal surgery has been identified by Rhee and coworkers (Rhee *et al.* 2011), noting that the subjective nature of assessment for nasal reconstruction surgery for nasal obstruction leads to a reported 25-50% failure rate. The objective of Rhee's work was to evaluate the ability of CFD to predict surgical outcomes to prove the utility of CFD modeling as part of a surgical planning procedure. It was found that virtual surgical procedures and CFD analysis for a patient undergoing inferior turbinate reduction and septoplasty provided good predictions of overall reduction in nasal resistance and flow distribution between the two sides of the nose. Kimbell and colleagues (Kimbell *et al.* 2013) furthered Rhee's work by simulating pre- and postoperative nasal geometries of ten patients who underwent various surgery to relieve nasal obstruction. They recorded moderate linear correlation with patient-reported outcomes for unilateral heat flux, unilateral airflow, and unilateral nasal resistance as a fraction of bilateral nasal resistance all calculated on the most obstructed side. These results suggest that the proposed metrics may be useful when planning surgical procedures of this kind. Finally, work by Hariri and colleagues (Hariri *et al.* 2015) employed CFD to predict if patients would benefit from turbinate reduction surgery and what surgical procedure would give the best results. They assessed nasal resistance, heat flux, and humidity transport and found that predicted outcomes from various procedures was specific to each patient's nasal geometry, emphasizing the need for customized surgical

planning. It was also found that the location of inferior turbinate resection, medial vs bottom resection, had little influence on nasal resistance, although nasal air conditioning was better preserved by bottom resection, emphasizing the importance of using multiple metrics to gauge surgical outcome. To be able to guide surgical intervention for ENS, one must identify objective measures that can be made using CFD or otherwise which correlate with the patients' symptoms. In the case of the patient's subjective sense of nasal obstruction, this is a difficult task.

Computational simulation has the potential to tackle our poor understanding of ENS. There still remains a paucity of computational investigation into ENS and it is clear that further investigation of patients suffering from the condition would benefit the medical community. Our ultimate goal is to address this by providing analysis of multiple patients suffering from ENS. We intend to focus on understanding paradoxical nasal obstruction specifically, by investigating correlation between fluid dynamic metrics obtained using CFD and subjective reports of nasal obstruction. This has not yet been investigated in patients that have suffered from ENS and have been corrected by reconstructive surgery. Using CFD to aid nasal surgical procedures has been gaining traction in the literature and has the potential to shift the current paradigm toward a predictive treatment. It is proposed in the current work that surgical planning be aided by automatic shape optimization of the interior surface of the nose in order to help the surgeon identify a procedure that will result in maximum improvement in patient-determined outcomes. All patients to be included in this work have provided permission for their CT scans to be used.

3. Methods

Methods presented here focus on the computational workflow that will be used to analyze the airflow within the nasal cavity.

Working closely with the Division of Rhinology & Endoscopic Skull Base Surgery, Department of Otolaryngology- Head & Neck Surgery at the Stanford University School of Medicine in Stanford CA, CT scans of patients suffering from ENS have been obtained with consent. One patient underwent surgery to restore normal nasal function and both pre- and postoperative scans are available (images from the preoperative scan are shown in Figure 2). A second patient also suffering from ENS who has undergone multiple surgical procedures and has performed a self-investigation on their condition will be consulted and investigated. Pre- and postoperative simulations of these patients' nasal cavities will be performed and compared to patient-specific outcomes in order to improve understanding of ENS.

The CT scans are used to construct a 3D geometry that will be employed in our CFD analysis in the future. The process of model construction is known as 3D-segmentation and involves separating voxels (3D pixels) in the CT data representing air from that of tissue. The voxels are separated by applying an intensity filter to the data with the air displaying a low intensity while tissue displays a high intensity. The particular method used here is known as thresholding (Figure 3).

Following a smoothing operation, the segmented image is then converted from a cloud of voxels into a 3D surface mesh, a STereoLithography (STL) file in this case. The surface mesh defines the boundary of the volume of interest and is required for the generation of the volume mesh. The entire process from CT to STL is facilitated by an open source software package known as 3D Slicer (Fedorov *et al.* 2012).

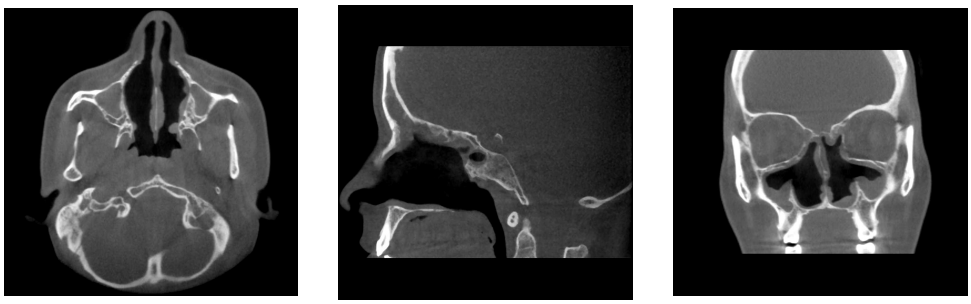

(a) Axial (b) Sagittal (c) Coronal

Figure 2: CT scans of patient suffering from ENS in the (a) axial, (b) sagittal, and (c) the coronal plane.

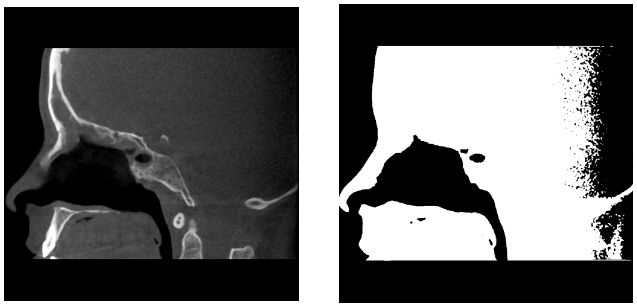

(a) Original (b) Threshold

Figure 3: The thresholding procedure filters the CT image by an intensity threshold, (a) the original CT image, (b) the image after thresholding; the black areas are all that remain.

The raw STL file is cropped to remove excess volume and is modified to include an entrance region outside the nose, while the trachea is extended to avoid interaction between the flow and the outlet boundary in the region of interest (Figure 4). This is performed by another open source software package, Meshmixer (Schmidt & Singh 2010). Meshmixer is also used to define the surface mesh that will be used for volume mesh generation. This package allows the mesh density to be modified depending on the surface detail required.

The produced STL files may contain erroneous surface definitions (Bohn & Wozny 1992). Such problems include self-intersecting facets and T-vertices which cannot be handled by volume mesh generators. To remedy these issues, yet another open source program is used, Meshlab (Cignoni *et al.* 2008), which has a number of tools for repairing geometry files such as these.

Unstructured, tetrahedral volume meshing is performed by Tetgen (Si 2013). Tetgen can be used as a standalone program, but in this case it is convenient to use Simvascular (SV-Development-Team 2014) as an interface. SimVascular provides some more advanced meshing options (Sahni *et al.* 2008) and allows the user to label mesh boundaries so that they can be recognized by the flow solver. This is the extent to which work has been completed thus far.

The Multi-Physics Finite Element Solver (MUPFES) (Esmaily-Moghadam 2014) will

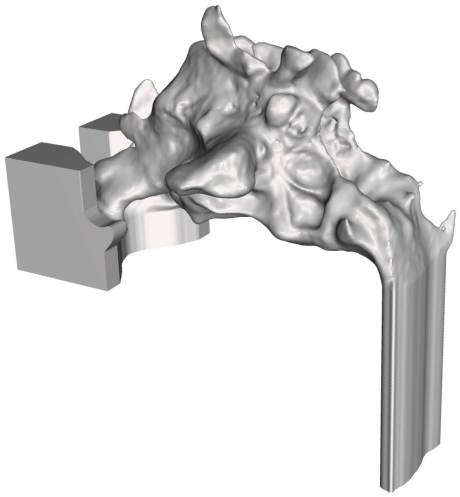

Figure 4: An STL surface mesh file is generated from the segmented CT scan and modified for simulation.

be used to solve the airflow through the nasal geometry. MUPFES uses a continuous Galerkin method to solve a wide variety of partial differential equations. In this case the time dependent, incompressible, Navier-Stokes equations along with advection-diffusion equations to describe heat and moisture transport in the nose are solved. At the low flow rates occurring in the upper airway, the assumption of incompressibility is reasonable. It has been shown that the air flow through the nose is mostly laminar (Doorly *et al.* 2008; Chung *et al.* 2006) and has been treated as such in many CFD simulations (Hariri *et al.* 2015; Di *et al.* 2013). Typical Reynolds numbers encountered in the nasal airway can range from 700 - 2400 (Girardin *et al.* 1983) depending on location. Some experimentalists have seen evidence for turbulence even at low flow rates (Girardin *et al.* 1983; Simmen *et al.* 1999). Due to the existence of the recirculation regions in the nasal cavity of patients with ENS, flow instabilities are more likely in our simulations, requiring a special care to ensure convergence of the results. This may involve comparison of our results against other high fidelity numerical solutions. The largest length and time scales relevant to this simulation, corresponding to the inlet-to-outlet chord-length and average fluid residence time, have been estimated to be on the order of 0.15m and 0.26s respectively with the ENS nasal cavity having an average hydraulic diameter of about 0.023m. The Kolmogorov length and time scales have been estimated to be on the order of $1x10^{-4}$m and $7x10^{-4}$s. Most of the nose's air conditioning function is undertaken during inspiration as it must warm and humidify the air before it reaches the lungs. Inspiration is of most interest with regard to nasal obstruction symptoms, and it has been shown that inspiration is much more sensitive to nasal geometry changes than expiration (Hörschler *et al.* 2006). Inspiration can be reasonably approximated as a steady problem (Keyhani *et al.* 1995). The present study will simulate inspiration with a constant volumetric flow rate of 250 ml/s corresponding to resting conditions (Tobin *et al.* 1983). The imposed boundary conditions include a zero pressure inlet on the external faces surrounding the nares, a volumetric flow rate outlet at the base of the nasopharynx, and a no-slip wall condition on the surfaces of the airway. Lindemann and others (Lindemann *et al.* 2002) determined

the temperature of the nasal mucosa during inspiration with room air nominally at 25°C and 30%RH. They found that the mucosa temperature varied from 30.2°C to 33.2°C depending on location during inspiration. The approach taken by the present study will be similar to that performed by Garcia and colleagues (Garcia *et al.* 2007), and a mean mucosa temperature of 31.7°C will be applied to the mucosa along with a 100% RH boundary condition while the room air will be simulated as 25°C and 30%RH.

4. Summary of current progress

At present a workflow has been developed to take CT scans through to a usable volumetric mesh. The most immediate tasks include undertaking a mesh independence study and comparing our flow solution to that of one including a turbulence model to ensure that we have a sufficiently well resolved solution. Through the process of obtaining a volume mesh from CT data, it is expected that there will be discrepancy between the modeled geometry and real life. These errors will most likely stem from the threshold intensity values selected during the segmentation of the CT data. For the results of this study to be meaningful, the effect of these errors on the flow solution must be evaluated. Once confidence of the accuracy of the solution is established, detailed comparison of pre- and postoperative simulations of the airways of patients' who suffered from ENS will be made. These results will be compared with current literature (Garcia *et al.* 2007) and used to generate hypotheses to aid prediction of patient symptoms. From here it is intended that shape optimization be considered as a tool to provide surgeons with surgical advice.

Acknowledgments

This work has been funded by Fulbright New Zealand.

REFERENCES

Bohn, J. H. & Wozny, M. J. 1992 Automatic CAD-model repair: Shell-closure. *Tech. Rep.* Rensselaer Design Research Center.

Chen, X., Leong, S., Lee, H., Chong, V. & Wang, D. 2010 Aerodynamic effects of inferior turbinate surgery on nasal airflow - A computational fluid dynamics model. *Rhinology* **48**, 394–400.

Chhabra, N. & Houser, S. M. 2009 The diagnosis and management of empty nose syndrome. *Otolaryng. Clin. N. Am* **42** (2), 311–330.

Chung, S.-K., Son, Y. R., Shin, S. J. & Kim, S.-K. 2006 Nasal airflow during respiratory cycle. *Am. J. Rhinol.* **20** (4), 379–384.

Cignoni, P., Corsini, M. & Ranzuglia, G. 2008 Meshlab: an open-source 3d mesh processing system. *ERCIM News* **73**, 45–46.

Coste, A., Dessi, P. & Serrano, E. 2012 Empty nose syndrome. *European Annals of Otorhinolaryngology, Head and Neck Diseases* **129**, 93–97.

Croce, C., Fodil, R., Durand, M., Sbirlea-Apiou, G., Caillibotte, G., Papon, J.-F., Blondeau, J.-R., Coste, A., Isabey, D. & Louis, B. 2006 In vitro experiments and numerical simulations of airflow in realistic nasal airway geometry. *Ann. Biomed. Eng.* **34** (6), 997–1007.

Di, M.-Y., Jiang, Z., Gao, Z.-Q., Li, Z., An, Y.-R. & Lv, W. 2013 Numerical

simulation of airflow fields in two typical nasal structures of empty nose syndrome: A computational fluid dynamics study. *PLoS ONE* **8** (12).

Doorly, D. J., Taylor, D. J., Gambaruto, A. M., Schroter, R. C. & Tolley, N. 2008 Nasal architecture: form and flow. *Philos. T. Roy. Soc. A* **366** (1879), 3225–3246.

Esmaily-Moghadam, M. 2014 Multi-Physics Finite Element Solver (MUPFES). *https://sites.google.com/site/memt63/MUPFES*

Fedorov, A., Beichel, R., Kalpathy-Cramer, J., Finet, J., Fillion-Robin, J.-C., Pujol, S., Bauer, C., Jennings, D., Fennessy, F., Sonka, M., Buatti, J., Aylward, S., Miller, J. V., Pieper, S. & Kikinis, R. 2012 3D Slicer as an image computing platform for the Quantitative Imaging Network. *Magn. Reson. Imaging* **30** (9), 1323–41.

Freund, W., Wunderlich, A. P., Stöcker, T., Schmitz, B. L. & Scheithauer, M. O. 2011 Empty nose syndrome: Limbic system activation observed by functional magnetic resonance imaging. *Laryngoscope* **121** (9), 2019–2025.

Garcia, G. J. M., Bailie, N., Martins, D. A. & Kimbell, J. S. 2007 Atrophic rhinitis : a CFD study of air conditioning in the nasal cavity. *J. Appl. Physiol.* **103**, 1082–1092.

Girardin, M., Bilgen, E. & Arbour, P. 1983 Experimental study of velocity fields in a human nasal fossa by laser anemometry. *Ann. Oto. Rhinol. Laryn.* **92** (3 Pt 1), 231–236.

Grützenmacher, S., Lang, C. & Mlynski, G. 2003 The combination of acoustic rhinometry, rhinoresistometry and flow simulation in noses before and after turbinate surgery: a model study. *ORL* **65** (6), 341–347.

Hariri, B. M., Rhee, J. S. & Garcia, G. J. M. 2015 Identifying patients who may benefit from inferior turbinate reduction using computer simulations. *Laryngoscope* pp. 1–7.

Hörschler, I., Brücker, C., Schröder, W. & Meinke, M. 2006 Investigation of the impact of the geometry on the nose flow. *Eur. J. Mech. B-Fluid.* **25** (4), 471–490.

Houser, S. M. 2007 Surgical treatment for empty nose syndrome. *Arch. Otolaryngol.* **133** (9), 858–863.

Jang, Y. J., Kim, J. H. & Song, H. Y. 2011 Empty nose syndrome: Radiologic findings and treatment outcomes of endonasal microplasty using cartilage implants. *Laryngoscope* **121**, 1308–1312.

Keyhani, K., Scherer, P. & Mozell, M. 1995 Numerical simulation of airflow in the human nasal cavity. *J. Biomech. Eng.-T. ASME* **117** (4), 429–441.

Kimbell, J. S., Frank, D. O., Laud, P., Garcia, G. J. M. & Rhee, J. S. 2013 Changes in nasal airflow and heat transfer correlate with symptom improvement after surgery for nasal obstruction. *J. Biomech.* **46** (15), 2634–2643.

Kuan, E. C., Suh, J. D. & Wang, M. B. 2015 Empty nose syndrome. *Curr. Allergy Asthm. R.* **15**, 493.

Lindemann, J., Leiacker, R., Rettinger, G. & Keck, T. 2002 Nasal mucosal temperature during respiration. *Clin. Otolaryngol.* **27**, 135–139.

Moore, E. J. & Kern, E. B. 2001 Atrophic rhinitis: a review of 242 cases. *Am. J. Rhinol.* **15** (6), 355–361.

Na, Y., Chung, K. S., Chung, S.-K. & Kim, S. K. 2012 Effects of single-sided inferior

turbinectomy on nasal function and airflow characteristics. *Resp. Physiol. Neurobi.* **180** (2-3), 289–297.

Naftali, S., Rosenfeld, M., Wolf, M. & Elad, D. 2005 The air-conditioning capacity of the human nose. *Ann. Biomed. Eng.* **33** (4), 545–553.

Payne, S. C. 2009 Empty nose syndrome: What are we really talking about? *Otolaryng. Clin. N. Am.* **42** (2), 331–337.

Rhee, J. S., Pawar, S. S., Garcia, G. J. M. & Kimbell, J. S. 2011 Toward personalized nasal surgery using computational fluid dynamics. *Arch. Facial Plast. S.* **13** (5), 305–10.

Sahni, O., Jansen, K. E., Shephard, M. S., Taylor, C. a. & Beall, M. W. 2008 Adaptive boundary layer meshing for viscous flow simulations. *Eng. Comput.* **24** (3), 267–285.

Scheithauer, M. O. 2010 Surgery of the turbinates and "empty nose" syndrome. *GMS Curr. Top. Otorhinolaryngol. Head Neck Surg.* **9**, Doc03.

Schmidt, R. & Singh, K. 2010 Meshmixer: an interface for rapid mesh composition. In *SIGGRAPH 2010*.

Si, H. 2013 TetGen - A quality tetrahedral mesh generator and a 3D delaunay triangulator. *Tech. Rep.*. Weierstrass Institute for Applied Analysis and Stochastics, Berlin.

Simmen, D., Scherrer, J. L., Moe, K. & Heinz, B. 1999 A dynamic and direct visualization model for the study of nasal airflow. *Arch. Otolaryngol.* **125** (9), 1015–1021.

Sofroniew, M. V., Howe, C. L. & Mobley, W. C. 2001 Nerve growth factor signaling, neuroprotection, and neural repair. *Annu. Rev. Neurosci.* **24** (1), 1193–1216.

Sozansky, J. & Houser, S. M. 2015 Pathophysiology of empty nose syndrome. *Laryngoscope* **125** (1), 70–74.

SV-Development-Team 2014 SimVascular.

Tobin, M. J., Chadha, T. S., Jenouri, G., Birch, S. J., Gazeroglu, H. B. & Sackner, M. A. 1983 Breathing patterns. 1: Normal subjects. *Chest* **84** (2), 202–205.

Wexler, D., Segal, R. & Kimbell, J. 2005 Aerodynamic effects of inferior turbinate reduction: Computational fluid dynamics simulation. *Arch. Otolaryngol.* **131**, 1102–1107.

Wu, X., Myers, A. C., Goldstone, A. C., Togias, A. & Sanico, A. M. 2006 Localization of nerve growth factor and its receptors in the human nasal mucosa. *J. Allergy Clin. Immun.* **118** (2), 428–33.

Zhao, K., Blacker, K., Luo, Y., Bryant, B. & Jiang, J. 2011 Perceiving nasal patency through mucosal cooling rather than air temperature or nasal resistance. *PLoS ONE* **6** (10), e24618.

Zhao, K., Jiang, J., Blacker, K., Lyman, B., Dalton, P., Cowart, B. J. & Pribitkin, E. A. 2014 Regional peak mucosal cooling predicts the perception of nasal patency. *Laryngoscope* **124** (3), 589–95.